

Fabrication and Characterization of Riociguat Loaded Bionanofibres as a Platform for Drug Delivery

S. N. KHARDE*¹, DR. SARAVANAN K.²

¹Research Scholar, Bhagwant University, Ajmer, Rajasthan, India

²Professor at Veer Kunwar College of Pharmacy, Bijnor, UP.

*Address for correspondence

College of Pharmaceutical Sciences, PIMS (DU), Loni, Tal: Rahata, Dist:

Ahmednagar, Maharashtra Pin 413736

Abstract:

Recently, drug-controlled release nanotechnology has gained special attention in biomedicine. Bionanofibres drug delivery systems are able to improve therapeutic efficacy, reduce toxicity, and increase patient compliance by delivering drugs at controlled rate over a period of time to the site of action. Poor solubility, erratic bioavailability and delivery challenges associated with Riociguat, which is commonly used in pulmonary hypertension treatment, are overcome by exploring electrospun Nanofibres technology. Ulvan nanofibres were created using the emulsion electrospinning process with polycaprolactone (PCL). Numerous experiments, including solubility, in-vitro drug release, drug release kinetics, scanning electron microscopy (SEM), differential scanning calorimetric (DSC), and Fourier transform infrared (FTIR) spectroscopy, were used to evaluate riciguat-bionanofibres. It is expected that the construct described here, with its simple fabrication, inexpensive cost, and frequent dosage, will offer a platform that can be customized for Riociguat on-demand delivery.

Keywords: Bionanofibres, Electrospinning Method, Riociguat, Ulvan, Stability, Drug release.

Introduction:

Nanofibres, generally defined as fibers with a diameter below 100nm ^[1, 2]. Because of their unique characteristics such as high surface area to-volume ratio, high tensile strength, low

coefficient of thermal expansion and high Young's modulus ^[3]. Nanofibres are different from microsized fibers with regard to their mechanical, optical and dimensional properties ^[4]. Bionanofibres mainly based on bio-based materials to process into nano-objects using chemical treatment on the cellulose based materials or polysaccharides ^[5]. Bionanofibres are an exciting new class of material and having a wide range of applications from medical to consumer products and industrial to high- tech applications such as drug delivery involves colonic drug delivery ^[6], for wound dressing^[7], air and liquid filtration, energy storage, composite, aerospace, battery separators, optical and chemical sensors.

Polymers are playing an important role in the world for a number of applications beginning from daily needs to defense and biomedical areas. Polymers obtained from different biorenewable resources are generally called as bio based polymers and they possess a well-defined structure such as natural fibers, starch, proteins etc. The most abundant natural polymer, polysaccharides are mostly derived from biomass and agricultural resources. ^[8]. Polysaccharide Nanofibres have widely used because of its availability, biocompatibility, their mechanical strength, naturally optimized structure, biodegradability, sustainability and environmental friendliness ^[9].

The complex anionic sulfated polysaccharide known as "ulvan" is taken from the cell walls of green seaweeds belonging to the *Ulva* genus. ^[10] Pharmacological studies have demonstrated that Ulvan possesses anticoagulant, antioxidant, antitumor, immunomodulating, and antihyperlipidemic activities. ^[11] Moreover, nanofibrous membranes based on ulvan were found to promote attachment and proliferation of osteoblasts maintaining cell morphology and viability. ^[12]

Efforts to produce electrospun fibers using ulvan as the sole polymer under different solvent systems and electrospinning parameters have not been successful so far due mainly to its poor rheological properties. Addition of biocompatible polymers, such as polyvinyl alcohol (PVA), polyethylene oxide (PEO), or polycaprolactone (PCL), in small amounts could improve the rheological properties and the charge carrying capacity of the ulvan electrospinning solution, which is crucial for fiber formation. Furthermore, the successful combination of ulvan with such polymers could contribute to its known beneficial pharmacological properties.

Materials and Methods

Material

Polycaprolactone (PCL) with a mean molecular weight of 14,000 g·mol⁻¹, Riociguat and all the solvents used for the electrospinning were obtained from Sigma Aldrich. Ethanol serves as the solvent.

Methods

Solutions of PCL and Ulvan with different concentrations ranging from 1-5 % w/v were prepared by dissolving in ethanol and stirring for 2 to 3 h. Riociguat with 3% (w/v) were dissolved in the different concentrations of PCL and Ulvan solution and the Nanofibres were prepared using the electrospinning apparatus. The drug and polymer solutions were loaded in 2 ml syringes with 24G (ID 0.55x0.25mm) needles connected to the positive terminal of a high voltage DC supply. The drug and polymer solutions were set at a flow rate of 0.5 mLh⁻¹ with the voltage set at 25kV at 17 cm distance from needle tip and the collector. The Riociguat loaded PCL and Ulvan Nanofibres were deposited onto an aluminium substrate wound around a rotary drum placed perpendicular to the needle. Computer interphased Lab view software was used to operate syringe pump to dispense the drug and polymer solution at a desired flow rate.

Table No. 1 Solubility Studies of Pure Riociguat, Electrospun Nanofibre-Based Solid Dispersions, and the Physical Mixture Containing Polycaprolactone (PCI)

Preparation of Physical Mixtures as Controls:

To create physical mixtures for comparison, the medication and polymer (% w/w) were simply triturated in a porcelain mortar to yield a composition identical to the solid dispersions. The mixtures were sieved after which they were placed in amber glass receptacles with lids.

Evaluation of Riociguat Nanofibres

Drug Entrapment Study

The UV spectrophotometer was calibrated to 252 nm and used to quantify the amount of drug in the transparent supernatant following centrifugation in order to calculate the amount of drug entrapment. For this, a drug calibration curve that is considered to be normal was plotted. The total quantity of drug added during preparation was then subtracted from the amount of drug in the supernatant (W). In actuality, (W-w) will reveal how much substance is contained in the particles.

Then percentage entrapment of a drug was calculated according to Equation

$$\% \text{ Drug Entrapment} = (W-w/W) \times 100$$

Free drug content in the supernatant, which is obtained after centrifuging the solid lipid suspension at (15,000 rpm for 20 min at 0°C using an ultra centrifuge), was used to evaluate efficiency. UV spectrophotometric measurement of the absorption was done at 252 nm.

Batch	Process	Drug (w/v) : Polymer (w/v) (% : %)	Theoretical drug content	
			Amount (mg)	Expressed (mg)
Riociguat	-	3:0	100	100
F1	Electrospinning	3:1	75	100
F2	Electrospinning	3:2	60	100
F3	Electrospinning	3:3	50	100
F4	Electrospinning	3:4	37.5	100
F5	Electrospinning	3:5	30	100
PM	Physical mixture	3:5	30	100

Characterization of Riociguat Nanofibres

Optical Microscopy

The pre-weighted sample (100 mg) of drug-loaded NFs was mixed with 1.0 ml of distilled water to test the spontaneous development of self-assembled structures. To achieve a homogeneous

dispersion, the mixture was then lightly manually shaken for 1-2 minutes at room temperature (22 °C). For the goal of producing the self-deposition, the dispersion was equilibrated for at least 10 minutes. The sample dilution was necessary to obtain accurate pictures. The development of the self-assembled was then imaged with an optical microscope.

Fourier Transform Infrared Spectroscopy

A Fourier transform infrared (FTIR) spectroscope and Single Reflection ATR crystal were used to confirm the drug-polymer interactions of NFs for the Riociguat, Ulvan, and PCl granules as well as the electrospun NFs. Spectra ($n = 3$) were scaled and standardized, and the analytical range was from 550 cm^{-1} to 4000 cm^{-1} .

Scanning Electron Microscopy

Different types of interactions, including secondary electrons, backscattered electrons, and distinctive X-rays, are produced when a finely focused electron beam is scanned across the surface of the sample in scanning electron microscopy (SEM). Images of the sample are developed from these impulses by detectors and shown on a cathode ray tube screen. The elements present in the features can then be quickly determined using EDS or WDS. The morphological, structural, and surface properties of the Nanofibres are usually observed using SEM.

X-ray Diffraction

The XRD analyses were done to determine Riociguat molecular composition. The samples were equally distributed throughout the sample cell. In the X-ray Diffractometer, the sample cell was inserted (BRUKER ECO D8). The samples were run through the 10-80 Hz spectrum of frequencies.

DSC

On a Q200 V 24.4 instrument used, DSC experiments were carried out using nitrogen atmosphere and a flow rate of 20 mL/min. Aluminum plates were used to heat the samples from -50°C to 200°C.

In Vitro Drug Release

A pre-determined size of electrospun Nanofibre ($1 \times 1 \text{ cm}^2$) was placed in 100 ml of phosphate buffer pH 6.8 to test the drug release from the Nanofibres. The release experiments were conducted in a thermostatic shaking incubator at 37 °C and 100 rpm. A UV-visible spectrophotometer (Lab India UV-3200) was used to measure the amount of drug in the aliquots at predetermined intervals with a maximum reading of 252 nm. Fresh media was then added to keep sink conditions.

Result and Discussion

Evaluation of Riociguat Nanofibres

Drug Entrapment Efficiency

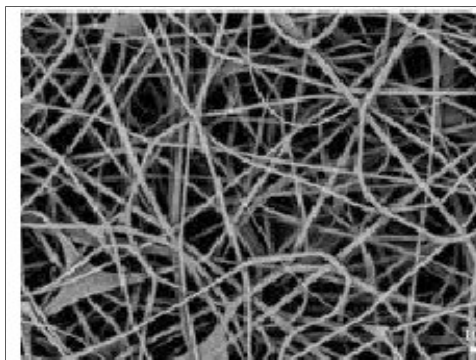
By using the dialysis technique, the entrapment effectiveness of Riociguat Nanofibre was evaluated. As the concentration of polymer increases, the efficiency of entrapment also increases. Based on the aforementioned findings, formulation F3, which has the highest percentage of entrapment efficiency (97%), was selected for additional study.

Table No. 2: Entrapment efficiency of Riociguat Nanofibre

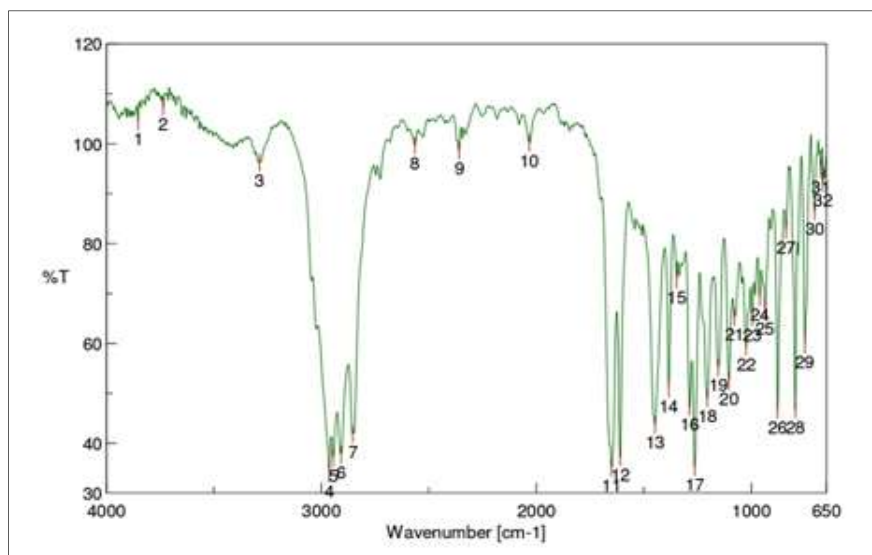
Formulation code	Entrapment Efficiency (%)
F1	90±0.12
F2	89±0.18
F3	97±0.13
F4	92±0.12
F5	93±0.05
PM	86±0.08

Characterization of Riociguat Nanofibres

Optical Microscopy

**Figure 1: Optical micrograph: Riociguat Nanofibres 100X**

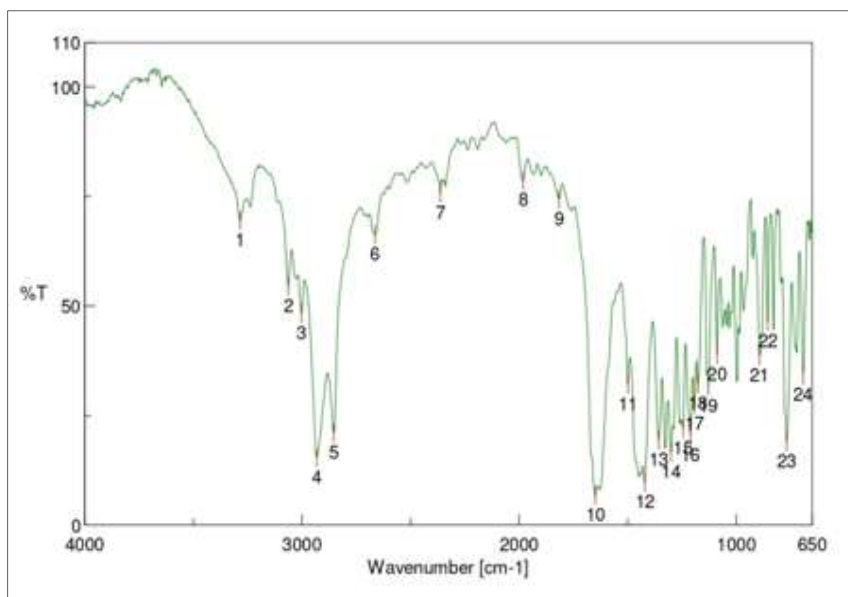
FTIR Studies



[Result of Peak Picking]

No.	Position	Intensity	No.	Position	Intensity
1	3853.08	104.422	2	3735.44	107.392
3	3288.04	96.2051	4	2963.09	33.8807
5	2944.77	36.9657	6	2908.13	37.6662
7	2854.13	41.8029	8	2564.86	99.59
9	2359.48	98.5585	10	2032.6	100.122
11	1649.8	35.0527	12	1610.27	37.1487
13	1447.31	43.6619	14	1383.68	50.9172
15	1348	72.7695	16	1287.25	47.3038
17	1263.15	35.145	18	1205.29	48.9995
19	1154.19	55.2027	20	1104.05	52.4195
21	1078.01	65.2779	22	1024.02	59.3509
23	996.053	65.1081	24	960.377	69.2606
25	936.271	66.4224	26	877.452	46.6234
27	838.883	82.7279	28	795.493	46.7
29	751.138	59.6987	30	705.819	86.4728
31	675.928	94.8964	32	667.25	92.1298

Figure 2: FTIR Spectra of Riociguat



[Result of Peak Picking]

No.	Position	Intensity	No.	Position	Intensity
1	3285.14	69.4409	2	3062.41	54.4446
3	3001.66	48.1934	4	2931.27	15.3071
5	2853.17	20.8739	6	2663.21	66.2157
7	2363.34	75.6481	8	1981.5	78.536
9	1815.65	74.2315	10	1648.84	6.6676
11	1498.42	31.9772	12	1421.28	9.76042
13	1357.64	19.3957	14	1300.75	16.4653
15	1245.79	22.0312	16	1211.08	20.3028
17	1192.76	27.4977	18	1176.36	32.0699
19	1128.15	31.6393	20	1088.62	38.8093
21	892.88	38.667	22	855.275	46.3792
23	767.53	18.9688	24	692.32	34.1568

Figure 3: FTIR Spectra of Riociguat with PCI, Ulvan polymer Compatibility

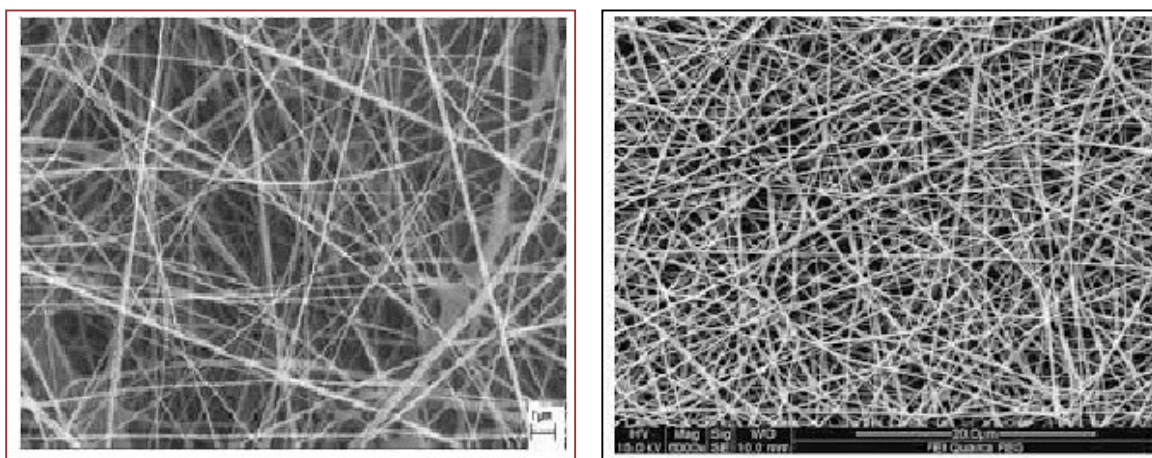


Figure 4 : SEM Analysis of Amphiphilic NFs and Templates of Riociguat

XRD Studies

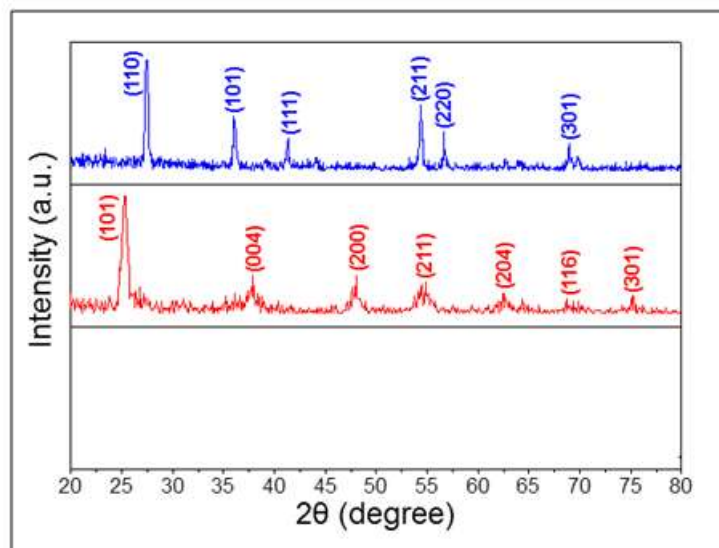


Figure 5: X-ray diffraction (XRD) patterns of Riociguat nanofibers

XRD was used to characterize Riociguat and Riociguat nanofibers in order to show the physical state of Riociguat in the nanofibers. Figure 5 shows XRD patterns of the Riociguat and Riociguat nanofibers. It shows peaks centered at 25.5, 37.9, 49.1, 55.2, 63.2, 68.8, and 76.2° corresponding to the (101), (004), (200), (211), (204), (116), and (301) planes of Riociguat. Representative XRD patterns of Riociguat Nanofibers are shown in Figure. It shows peaks located at 27.5, 36.2, 41.3, 54.4, 56.7, and 69.2°, which can be attributed to the (110), (101), (111), (211), (220), and (301) planes of Nanofibers.

DSC Study

Thermal behavior of Riociguat nanofibers was analyzed by using DSC-Q200 for a temperature range of -50°C to 200°C. Two Electrospun samples of voltage 18 kV and 30 kV were selected to study their thermal properties. These samples represented morphologies of nanofibers and their thermograms can be observed in figures. Both the samples at 18 kV and 30 kV had the same T_g and their melting points (T_f) were almost same at 58.25°C and 58.43°C but their crystallinity ration was increased to 48% and 50% respectively.

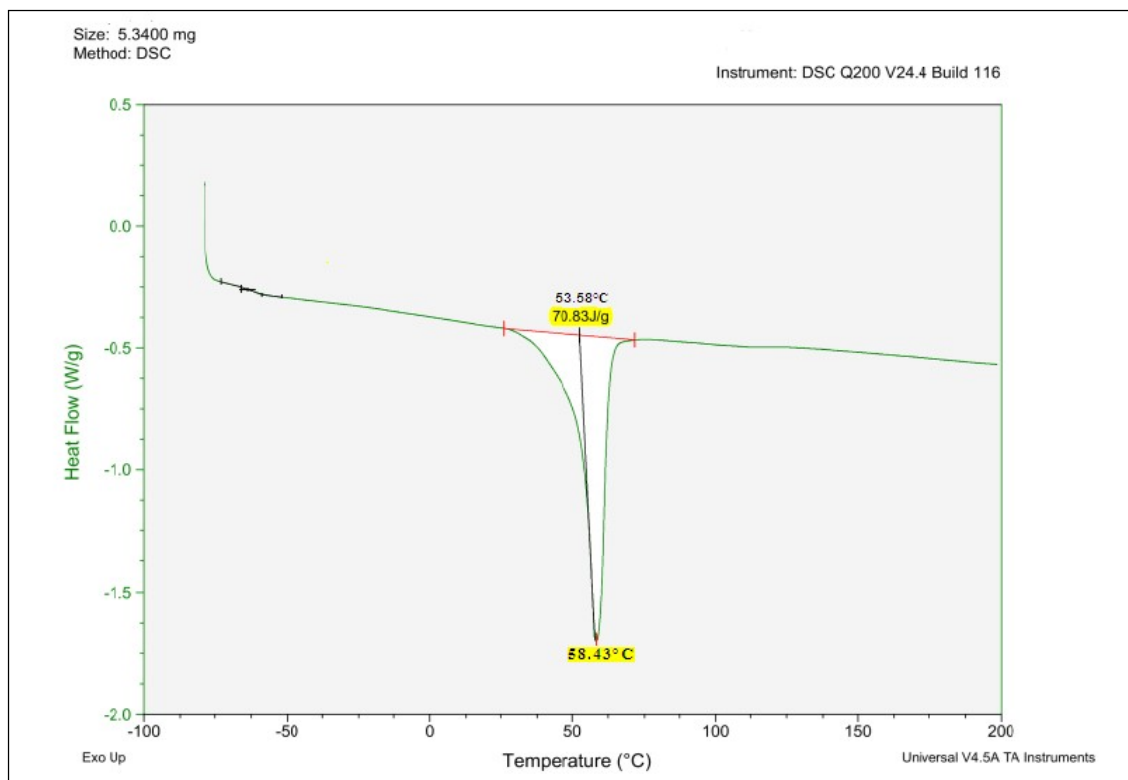


Figure 6 : DSC study of Riociguat Nanofibers at 18 kV

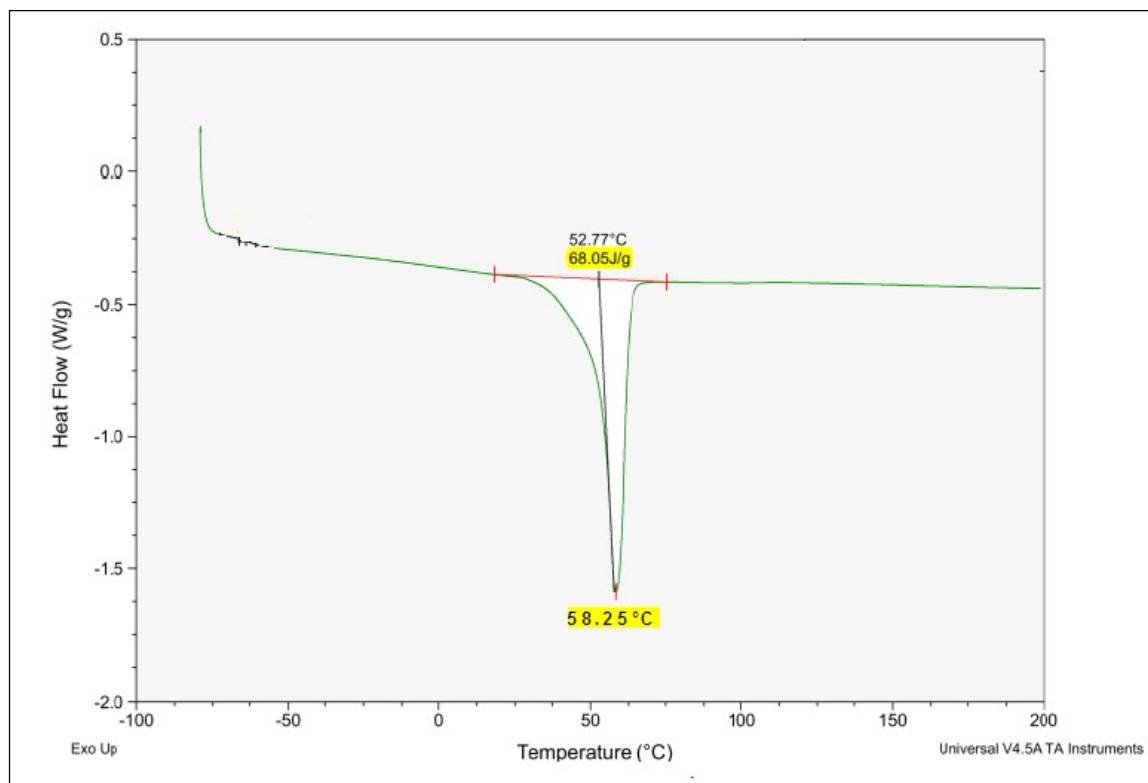


Figure 7: DSC study of Riociguat Nanofibers at 30 kV

In Vitro Drug Release of Riociguat Nanofibres

Figure 8 displays the total dissolution profiles of Riociguat loaded into the F3 amphiphilic electrospun NFs formulation. Within the first two hours, more than 50% of Riociguat was released, followed by about 80% in the following two hours, and the remainder (100%) of the active substance was released within 30 hours (Figure 8). The surface or near surface distribution of Riociguat in the nano fibres may have contributed to the original burst release of the drug-loaded amphiphilic nano fibres. As a consequence, the nanofibrous template swells. Only comparing the dissolution characteristics of the current amphiphilic nanofibrous templates loaded with the active agent is the purpose of our dissolution research.

Table 3: Invitro Drug Release of Riociguat Nanofibres

Time in (Hr)	% Drug Release of F3
0	0
1	6.73±0.08
2	8.74±0.12
3	11.42±2.01
4	21.63±1.27
5	37.82±2.23
6	46.31±1.43
12	54.27±1.34
18	67.31±2.78
24	73.22±2.23
48	94.37±2.22

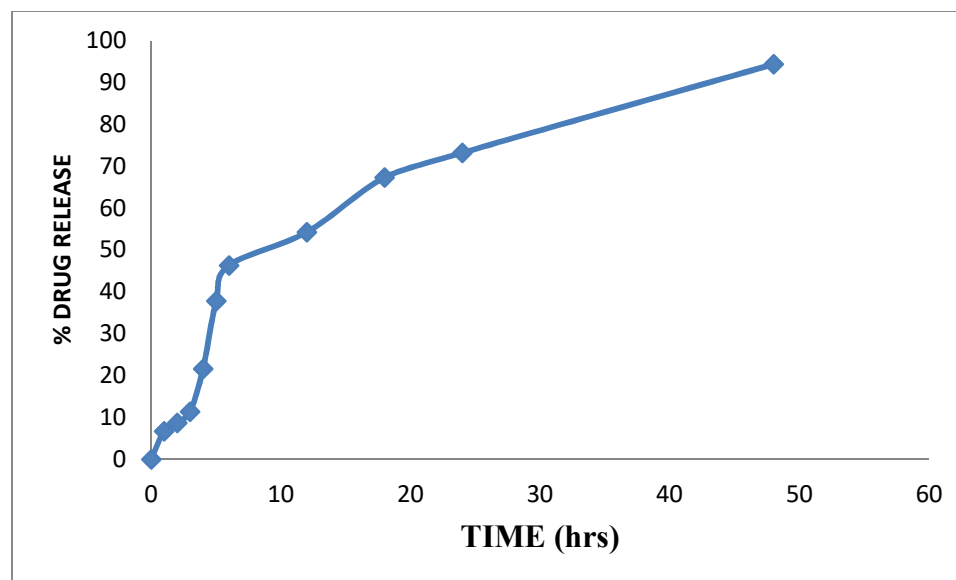


Figure 8: In Vitro dissolution profiles of Riociguat -loaded amphiphilic Electrospun NFs formulation F3.

Conclusion:

In the current study, bionanofibres were successfully generated using the electrospinning method. By using SEM and FTIR, among other methods, the chemical structure, morphology, and thermal durability of bionanofibres were studied. The findings of the FTIR measurements show that there is no interaction between the medications and the polymers. According to SEM research, DSC shows that Ulvan may manufacture NFs using Polycaprolactone (PCL), a well-known and efficient carrier polymer. Following drug injection, the surface area and roughness of the nanofibers reduced. The drug was released from bionanofibres in a controlled manner, according to the in-vitro action. Therefore, the present study confirms the possibility of drug delivery through Nanofibres at the intended site.

Reference:

1. Khan P. A., Sasikanth K., Nama S., Suresh S., Brahmaiah B. Nanofibres- A new trend in nano drug delivery systems. *PharmaInnov J.* 2013; 2(2): 118-127.
2. Potti L., Kattamuri B. K., Vinukonda A., et al. Nanofibres in pharmaceuticals – A Review. *Am J PharmTech Res.* 2012; 2(6): 188-212.
3. Chirayli C. J., Mathew L., Thomas S. Review of recent research in nano cellulose preparation from different lignocellulosic fibers. *Rev Adv Mater Sci.* 2014; 37: 20-28
4. Dutta A. K., Kawamoto N., Sugino G., Izawa H., et al. Simple preparation of Chitosan Nanofibres from dry chitosan powder by the Star Burst System. *CarbohydrPolym.* 2013; 97: 363-367
5. Kondo T., Kose R., Naito H., Kasai W. Aqueous counter collision using paired water jets as a novel means of preparing bioNanofibres. *CarbohydrPolym.* 2014; 112: 284- 290

6. Akhgari A., Heshmati Z., Makhmalzadeh B. S. Indomethacin electrospun Nanofibres for colonic drug delivery: Preparation and characterization. *Adv Pharm Bull.* 2013; 3(1): 85- 90
7. Chellamanik P., Balaji R. S., Veerasubramanian D. Development of wound dressing made of electrospun tetracycline hydrochloride drug incorporated PCL [Poly (E- Capro lactone)] nanomembrane. *Int J EngAdv Technol.* 2014; 4(4): 251-256
8. Thakur V. K., Thakur M. K., “Processing and characterization of natural cellulose fibers/thermoset polymercomposites”, *Carbohydrate Polymers*, 109: 102-117, 2014.
9. Motonari S., Tsubouchi G., Nakamura M., Hayashi M., “Polysaccharide Nanofibre made from euglenoid alga”, *Carbohydrate Polymers*, 93: 499-505, 2013.
10. Lahaye M, Robic A. Structure and functional properties of ulvan, a polysaccharide from green seaweeds. *Biomacromolecules.* 2007 Jun 11;8(6):1765-74.
11. Patel S. Therapeutic importance of sulfated polysaccharides from seaweeds: updating the recent findings. *3 Biotech.* 2012 Sep;2(3):171-85..
12. Toskas, G.; Heinemann, S.; Heinemann, C.; Cherif, C.; Hund, R. D.; Roussis, V.; Hanke, T. *Carbohydr. Polym.* 2012, 89, 997.
13. Bölgen N, Vargel I, Korkusuz P, Menciloğlu Y Z, Pişkin E. In vivo performance of antibiotic embedded electrospun PCL membranes for prevention of abdominal adhesions. *J. Biomed. Mater. Res. Part B Appl. Biomater.* 2010 ;81B:530–543.
14. Huang Z M, Yang C L. Encapsulating drugs in biodegradable ultrafine fibers through co-axial electrospinning. *J. Biomed. Mater. Res. Part A* 2010 ;77A :169–179.
15. Kim K, Luu Y K, Chang C, Fang D, Hsiao B S, Hadjiargyrou M. Incorporation and controlled release of a hydrophilic antibiotic using poly(lactide-co-glycolide)-based electrospun nanofibrous scaffolds. *J. Control. Release* 2004; 98: 47–56.
16. Nie H, Wang C H. Fabrication and characterization of PLGA/HAp composite scaffolds for delivery of BMP-2 plasmid DNA. *J. Control. Release* 2007; 120: 111–121.
17. Chew S Y, Jie W, Yim E K, Leong K W. Sustained release of proteins from electrospun biodegradable fibers. *Biomacromolecules* 2005; 6:2017–2024.
18. Sadeghi A, Moztarzadeh F, Aghazadeh M J. Investigating the effect of chitosan on hydrophilicity and bioactivity of conductive electrospun composite scaffold for neural tissue engineering. *Int. J. Biol. Macromol.* 2019;121: 625–632.
19. Venugopal E, Rajeswaran N, Sahanand K S, Bhattacharyya A, Rajendran S. In vitro evaluation of phytochemical loaded electrospun gelatin Nanofibres for application in bone and cartilage tissue engineering. *Biomed. Mater.* 2018; 14: 015004.
20. Ding Y, Li W, Zhang F, Liu Z, Zanjanzadeh E N, Liu D, Santos H A Electrospun fibrous architectures for drug delivery, tissue engineering and cancer therapy. *Adv. Funct. Mater.* 2019; 29: 1802-1832.
21. Sill T J, Von Recum H A. Electrospinning: Applications in drug delivery and tissue engineering. *Biomaterials* 2008; 29: 1989–2006.

22. Kenawy E R, Bowlin G L, Mansfield K, Layman J, Simpson D G, Sanders E H, Wnek G E. Release of tetracycline hydrochloride from electrospun poly(ethylene-co-vinylacetate), poly(lactic acid), and a blend. *J. Control. Release* 2002; 81:57–64.
23. Park K, Ju Y M, Son J S, Ahn K D, Dong K H. Surface modification of biodegradable electrospun Nanofibre scaffolds and their interaction with fibroblasts. *J. Biomater. Sci. Polym. Ed.* 2007; 18:369–382.
24. Ye K, Liu D, Kuang H, Cai J, Chen W, Sun B, Xia L, Fang B, Morsi Y, Mo X. Three-dimensional electrospun nanofibrous scaffolds displaying bone morphogenetic protein-2-derived peptides for the promotion of osteogenic differentiation of stem cells and bone regeneration. *J. Colloid Interface Sci.* 2019; 534: 625–636.
25. Chen R, Wang J, Liu C. Biomaterials act as enhancers of growth factors in bone regeneration. *Adv. Funct. Mater.* 2016; 26:8810–8823.